Armenian Journal of Physics, 2019, vol. 12, issue 3, pp. 254-260

Magnetic Properties of the Octanuclear Nickel Phosphonate-Based Cage

(Proceedings of the Int. Conference on "The Problems of Modern Condensed Matter Physics")

Hamid Arian Zad[1,2], Azam Zoshki[3], Nerses Ananikian[4,5]

[1]*Alikhanyan National Science Laboratory, Alikhanian Br. 2, 0036 Yerevan, Armenia,*
[2]*ICTP, Strada Costiera 11, I-34151 Trieste,*
[3]*Young Researchers and Elite Club, Mashhad Branch, Islamic Azad University, Mashhad, Iran*
[4]*Alikhanyan National Science Laboratory, Alikhanian Br. 2, 0036 Yerevan, Armenia,*
[5]*CANDLE Synchrotron Research Institute, Acharyan 31, 0040 Yerevan, Armenia*
E-mail: arianzad.hamid@mail.yerphi.am

Received: 30 June 2019

Abstract. The magnetic and thermodynamic properties of the transition metal Ni^{II} phosphonate-based cage is reported in detail. The model is known as octanuclear nickel phosphonate cage $[Ni_8(\mu_3-OH)_4(OMe)_2(O_3PR_1)_2(O_2C^tBu)_6(HO_2C^tBu)_8]$ with the geometry of butterfly-shaped molecular structure in the presence of an external magnetic field. Firstly, using full exact diagonalization (ED) and quantum Monte Carlo simulations, we verify the model without aniostropic terms in order to compare our results with that of the original experimental data expressed in Refs. [18,19]. Then, we consider Heisenberg exchange anisotropy between interacted nickel atoms, besides an uniaxial single-ion anisotropy property for all of them, and examine effects of the both anisotropy parameters on the magnetization process also the specific heat of the model. Interestingly, we see some intermediate magnetization plateaus including 0-plateau, and magnetization jumps accompanying with the magnetic ground-state phase transitions at low temperature $T = 1\text{K}$. The magnetization plateaus are strongly dependent on the exchange anisotropy, as well as, single-ion anisotropy parameters. Actually, altering the exchange anisotropy leads to change in width and magnetic position of all intermediate plateaus.

Keywords: Magnetization plateaus, Specific heat, Phase transition, Nickel cage

1. Introduction

Obtaining a profound perception about interacting quantum systems like low-dimensional magnetic materials with competing interactions or geometrical frustration have become an intriguing research object in condensed matter physics, material science and chemistry [1, 2, 3, 4, 5]. In these particular areas many investigations concerned about metal containing compounds have been carried out, due to that they present a relevant combination of ferromagnetic and antiferromagnetic phases. As a result of zero- and low-temperature phase transitions, these systems manifest various ground-state phase diagrams, magnetic and thermal properties [5, 6, 7, 8, 9, 10, 11, 12, 13]. For instance, the analytical study of magnetic properties of the nickel homometallic magnetic compound $\left[Ni_3(fum)_2(\mu_3-OH)_2(H_2O)_4\right]_n.\ (2H_2O)_n$, indicating the coexistence of both antiferromagnetic and ferromagnetic interactions from experimental data[14] on a diamond chain have been carried out for low temperatures[15, 16, 17].

Single molecular magnets can be count as intriguing small spin clusters among these systems that have attracted appreciable interest during the current decade, owing to the fact that they can be plausibly characterized by the Heisenberg models [18, 19, 20, 21, 23, 24, 25, 26, 27, 28]. Polynuclear complexes involving transition-metal and lanthanide-metal ions synthesized from either identical or different metal ions are of increasing interest in molecular magnetism. In the

past two decades, it has become possible to synthesize a large variety of compounds including identical transition-metal ions with the geometry of butterfly-shaped subunit structures, which can be properly introduced in terms of Heisenberg models such as: $\left[Fe_6^{III}(\mu_3-O)_2(\mu-OH)_2\{\mu-(C_6H_{11})_2PO_2\}_6(\mu-tBuCO_2)_6(\eta_1-OH_2)_2\right].2CH_3CN.CH_2CL_2\right]$ (for more details see Ref. [21]), and nickel containing complex $\left[Ni_8(\mu_3-OH)_4(OMe)_2(O_3PR_1)_2(O_2C^tBu)_8\right]$ [18, 19].Also, several nickel containing compounds consisting of mixed transition-metal ions have widely been synthesized by scientists, for instance: heterometallicoctanuclear $Ni_4^{II}Ln_4^{III}(Ln=Y,Gd,Tb,Dy,Ho,\text{and } Er)$ complexes containing two butterfy-shaped $Ni_2^{II}Ln_2^{III}O_4$ [23], and heterometallic $(3\times3)-$grid $M^{II}Cu_4^{II}Cu_4^{I}(M=Ni,Cu,\text{and } Zn)$ reported in Ref. [22].

From quantum statistical mechanics view point, phase transitions at zero temperature where the quantum fluctuations play essential role, may describe the nature of materials in the real world, hence quantum phase transitions have been one of the most interesting topics to study various spin models [29, 30, 31, 32, 33, 34, 35, 36]. Further studies of quantum spin models have provided precise outcomes for the ground-state phase transition in the presence of an external magnetic field, which can be induced through the exchange couplings [37, 38, 39, 40]. Zero- and low-temperature magnetization curves of small spin clusters consisting of transition-metals are topical issue of current research interest, in order to they often involve a lot of intriguing features such as fractional magnetization (quasi) plateaus, magnetization jumps and magnetization ramps [24, 25, 26, 27, 28].

Since, anisotropy effects can substantially modify or control the ground-state properties of magnetic systems [41, 42], in the present work, we examine the low-temperature magnetization process and the specific heat of the octanuclear nickel phosphonate cage $\left[Ni_8(\mu_3-OH)_4(OMe)_2(O_3PR_1)_2(O_2C^tBu)_6(HO_2C^tBu)_8\right]$ in the presence of an external magnetic field by assuming aditional anisotropic terms: Heisenberg exchange anisotropies Δ_1 and Δ_2, also single-ion anisotropy D. To investigate the low-temperature magnetization behavior, as well as, isothermal specific heat of the considered nickel complex discussed above, we utilize exact numerical diagonalization method to diagonalize the Hamiltonian of the model. To ensure the correctness and completeness, we compare our exact results of magnetization process with those obtained through Quantum Monte Carlo (QMC) method. Actually, we use the subroutine $dirloop-sse-$ a package from the Algorithms and Libraries for Physics Simulations (ALPS) project. This provides a full generic implementation of the QMC procedure called the directed loop algorithm in the Stochastic Series Expansion representation [43, 44].

The paper is organized as follows. In Sec. 2. We introduce the exactly solvable model. In Sec. 3, we discuss the low-temperature magnetization process and specific heat of the model under consideration by assuming anisotropy properties. Some conclusions and future outlooks are briefly mentioned in Sec. 4.

2. Model

Hamiltonian of the octanuclear nickel phosphonate-based cage $\left[Ni_8(\mu_3-OH)_4(OMe)_2(O_3PR_1)_2(O_2C^tBu)_6(HO_2C^tBu)_8\right]$ shown in Fig. 1 can be expressed as

$$\begin{aligned} H = &-J_1\left[S_1\cdot S_2 + S_3\cdot S_4 + S_5\cdot S_6 + S_7\cdot S_8\right]- \\ &-J_2\left[S_1\cdot S_3 + S_2\cdot S_3 + S_4\cdot S_5 + S_4\cdot S_6 + \right. \\ &\left.+S_5\cdot S_7 + S_6\cdot S_7 + S_1\cdot S_8 + S_2\cdot S_8\right]- \\ &-g\mu_B B\sum_{j=1}^{8} S_j^z + D\sum_{j=1}^{8}\left(S_j^z\right)^2, \end{aligned} \tag{1}$$

First and second parts in equation (1) correspond to the anisotropic Heisenberg couplings between each pair spins interacted together, which is explicitly given by

$$\left(S_i\cdot S_j\right)_{J,\Delta} = J\left(S_i^x S_j^x + S_i^y S_i^y\right) + \Delta S_i^z S_i^z, \tag{2}$$

where $J=\{J_1,J_2\}$ denotes isotropic coupling constants, and $\Delta=\{\Delta_1,\Delta_2\}$ corresponds to the anisotropy exchange interactions. S^α for which $\alpha=\{x,y,z\}$ are spin-1 operators (with ħ = 1). B is the applied homogeneous magnetic field in the $z-$direction. The gyromagnetic ratio would be taken as $g=2.42$ [18] in the plots drawn in this paper. The characterization of the partition function of the model under consideration can be defined as $Z=Tr[\exp(-\beta H)]$, where $\beta=\dfrac{1}{k_B T}$, k_B is the Boltzmann's constant and T is the temperature.The Gibbs free energy can be obtained from the partition function of the system as $f=-k_B T\ln Z$.

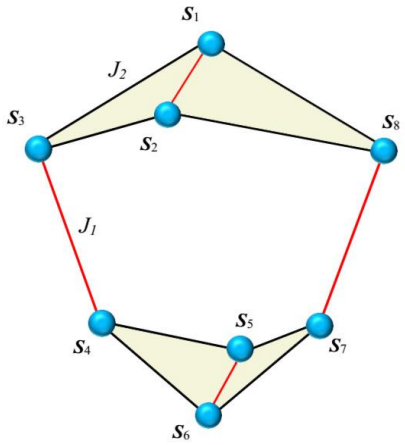

Figure 1: Schematic structure of the Heisenberg octanuclear nickel phosphonate cage. The balls denote Ni atoms that are connected together via Body-Body (BB) interdimer interaction $\boldsymbol{J_1}$and the corresponding Wing-Body (WB) interdimer interaction $\boldsymbol{J_2}$.

3. Results and Discussion

The following section introduces the most interesting results obtained from the study of the magnetization process, magnetic susceptibility, and specific heat of the butterfly-shaped octanuclear cluster $\left[Ni_8(\mu_3-OH)_4(OMe)_2(O_3PR_1)_2(O_2C^tBu)_6(HO_2C^tBu)_8\right]$ by utilizing the thermodynamic relations as following

$$M=-\left(\frac{\partial f}{\partial B}\right)_T, \quad \chi=\left(\frac{\partial M}{\partial B}\right)_T, \quad C=-\left(\frac{\partial^2 f}{\partial T^2}\right)_B. \tag{3}$$

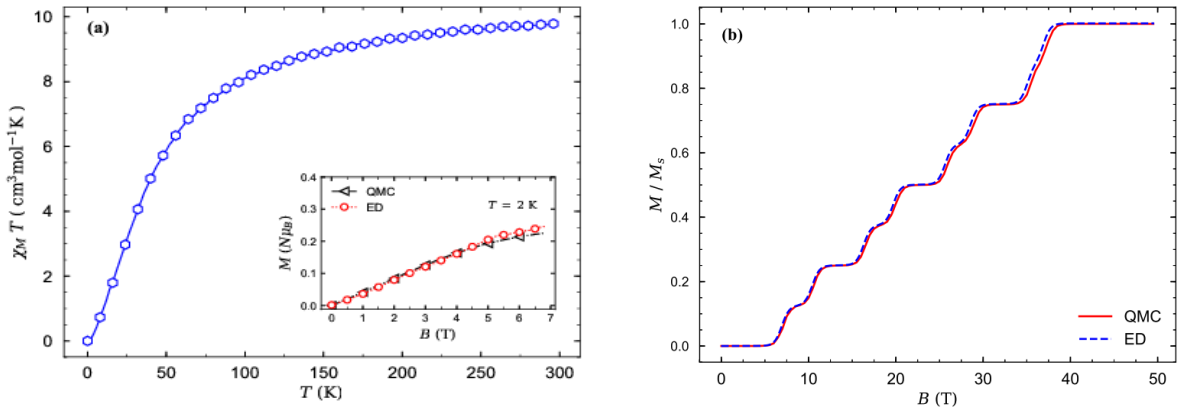

Figure 2: (a) QMC results for The temperature dependence of the product of magnetic susceptibility times the temperature $\boldsymbol{\chi_M T}$ for the Heisenberg octanuclear nickel phosphonate-based cage in the absence of the magnetic field ($\boldsymbol{B=0}$) for fixed values of $\boldsymbol{J_1=7.6\,cm^{-1}}$ and $\boldsymbol{J_2=-22.4\,cm^{-1}}$. The inset shows deduced magnetization per saturation $\boldsymbol{M/M_s}$ by QMC simulation and ED method as a function of the external magnetic field $\boldsymbol{B}$ for fixed values of $\boldsymbol{J_1=7.6\,cm^{-1}}$, $\boldsymbol{J_2=-22.4\,cm^{-1}}$ at moderate temperature $\boldsymbol{T=2}$ K. Due to compare with the experimental data in Ref. [18], other parameters have been taken as $\boldsymbol{\Delta_1=J_1}$, $\boldsymbol{\Delta_2=J_2}$ and $\boldsymbol{D=0}$. (b) The ED and QMC results for the magnetization per saturation value of the model versus magnetic field at low temperature $\boldsymbol{T=1\,K}$ for the same fixed values of other parameters as panel (a) divided by $\boldsymbol{\kappa_B}$, namely, $\boldsymbol{J_1/\kappa_B=7.6\,K}$ and $\boldsymbol{J_2/\kappa_B=-22.4\,K}$.

Figure 2(a) illustrates the QMC results of the temperature dependencies of the product of zero-field magnetic susceptibility times the temperature $\chi_M T$ of the model calculated by ALPS project. By comparing our numerical results and the experimental data expressed in Refs. [18, 19], we find that our results are in an excellent agreement with their experimental measurements. The room temperature $\chi_M T$ value for the model under consideration is 10.0 $cm^3 mol^{-1} K$ for the set of other parameters as $J_1=7.6cm^{-1}$, $J_2=-22.4cm^{-1}$ and $g=2.4$, which is close to the expected value 9.96 $cm^3 mol^{-1} K$ for eight isolated Ni^{II} ions. We note that in this step, we consider the model as a pure Heisenberg spin-1 cluster system isolated from any anisotropy dependencies. The inset of Fig. 2(a) displays the ED and QMC results for the magnetization versus magnetic field at moderate temperature $T=2K$ and the same set of coupling constants considered for examining $\chi_M T$. One can see from the inset that, not only ED and QMC results are in accordance with each other, but also they are in a good agreement with the experimental results reported in Ref. [18].

Figure 2(b) shows deduced magnetization per saturation value M/M_S from the ED and QMC methods as a function of the magnetic field at low temperature $T=1K$ for fixed values of $J_1/\kappa_B=7.6K$, $J_2/\kappa_B=-22.4K$ and $g=2.4$. We mention that in order to reduce the complexity of our numerical calculations, we change the units of exchange couplings into the temperature unit (Kelvin). The system has a complex magnetization scenario due to multiplicity of intermediate magnetization plateaus. It is quite obvious that the magnetization curve shows intermediate plateaus at $0, \frac{1}{8}, \frac{1}{4}, \frac{2}{5}, \frac{1}{2}, \frac{2}{3}$, and $\frac{3}{4}$ of the saturation magnetization. The large

number of magnetization plateaus is due to existence of a strong interdimer antiferromagnetic interaction $J_2/\kappa_B = -22.4K$. This figure also manifests a plausible coincidence between results of the both ED and QMC procedures.

Now, let us investigate the magnetization process and the specific heat of the model when it involves with the Heisenberg exchange anisotropies Δ_1 and Δ_2, as well as, single-ion anisotropy property D.Typical dependencies of the magnetization per saturation value are plotted in Fig. 3(a) against magnetic field B for different selected values of the single-ion anisotropy parameter D/κ_B, when the isotropic XXX Heisenberg case is considered for the model, namely, $\Delta_1/\kappa_B = J_1/\kappa_B = 7.6K$ and $\Delta_1/\kappa_B = J_2/\kappa_B = -22.4K$. Interestingly, the single-ion anisotropy variations have no remarkable influence on the magnetic dependence of magnetization in the magnetic field interval $B \le 20T$, where a magnetization jump occurs between $\frac{2}{5}-$plateau and $\frac{2}{5}-$ plateau (accompanying with the ground-state phase transition between plateaus $\frac{2}{5}$ and $\frac{1}{2}$ of the saturation magnetization). As a matter of fact, for the magnetic field range $B > 20T$, intermediate magnetization plateaus at $M/M_S \ge \frac{1}{2}\left(\frac{1}{2}, \frac{2}{3}, \text{and } \frac{3}{4} \text{ of the saturation magnetization}\right)$ become wider and shift toward stronger magnetic fields. Generally, there is a delay in the magnetization behavior to reach its saturation when the single-ion anisotropy increases.

To understand the spin exchange anisotropy effects on the magnetization process of the octanuclear nickel phosphonate cage, we plot in Fig. 3(b) the magnetization per saturation value M/M_S with respect to the magnetic field for various fixed values of the both exchange anisotropies Δ_1 and Δ_2, and optional value $D/\kappa_B = 10K$ at low temperature $T = 1K$. Coupling constants J_1 and J_2 have been taken as panel 3(a). As could be expected, the width and magnetic position of all plateaus undergo significant changes upon altering anisotropies. To clarify this point, the magnetization scenario for relatively small anisotropies $\Delta_1 \ll J_1$ and $|\Delta_2| \ll |J_2|$ is illustrated in Fig.3(b) on a particular example with $\Delta_1/\kappa_B = 1K$ and $\Delta_2/\kappa_B = -2K$ (red dot line).

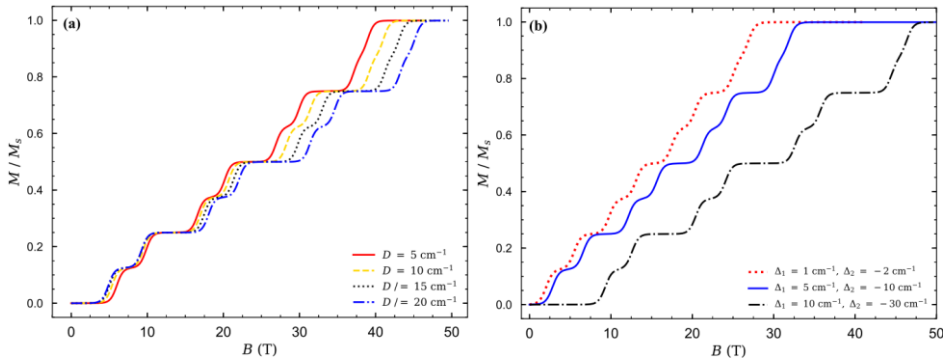

Figure 3: (a) ED results for the magnetization per saturation value M/M_S of the isotropic octanuclear nickel phosphonate-based cage as a function of the magnetic field B at low temperature $T = 1\ K$ for several fixed values of the single-ion anisotropy parameter D, by assuming fixed values of $J_1/\kappa_B = \Delta_1/\kappa_B = 7.6\ K$, and $J_2/\kappa_B = \Delta_2/\kappa_B = -22.4\ K$. (b) Magnetization per saturation value M/M_S as a function of the magnetic field at low temperature $T = 1\ K$ for different fixed values of exchange anisotropies Δ_1 and Δ_2, by assuming an optional value $D/\kappa_B = 10\ K$.

One can see that, the width of all plateaus becomes narrower and their magnetic positions shift toward lower magnetic fields. Consequently, the magnetization reaches its saturation value in lower magnetic fields (in this case $B_S \approx 28T$). For the case $\Delta_1 < J_1$ and $|\Delta_2| < |J_2|$ (blue solid line) wider magnetization plateaus are presented by magnetization curve, whose magnetic positions are in the stronger magnetic fields. When we consider high amounts of exchange anisotropies for the model such that $\Delta_1 > J_1$ and $|\Delta_2| > |J_2|$ (black dashed-dot line), the width of all magnetization plateaus considerably increase and their magnetic positions move to stronger magnetic fields, so the magnetization reaches its saturation value in the stronger magnetic fields (for this case $B_S \approx 45T$).

4. Conclusions

In this paper, we have theoretically investigated the magnetic and thermodynamic properties of the octanuclear nickel phosphonate-based cage with the geometry of butterfly-shaped molcular structure. To this end, we have examined the magnetization processes of the described model without anisotropy through ED and QMC methods. By comparing our results with the corresponding experimental data, we realized that they are in an excellent agreement with each other. Hence, we have continued our investigations by means of ED procedure for the magnetization process, as well as, the specific heat of the model including Heisenberg exchange anisotropy and single-ion anisotropy properties.

According to our investigations, we understood that the model has a complex magnetization scenario with a lot of intermediate plateaus and magnetization jumps at low temperature accompanying with the ground-state phase transitions. As a result, we found that the magnetization behavior rigorously depends on the Heisenberg exchange anisotropy and single-ion anisotropy properties. Actually, there is a typical competition between spin exchange anisotropies and the single-ion anisotropy to alter the width and magnetic position of the magnetization plateaus. Strong single-ion anisotropy leads to increase the width of intermediate magnetization plateaus, also shift their magnetic positions toward stronger magnetic fields.

Further studies about the effects of anisotropies on the cooling/heating and magneticaloric process of the octanuclear nickel phosphonate-based cage and/or similar small spin clusters can be very intriguing topics, that would be the subject of our future works.

Acknowledgements

H. Arian Zad and N. Ananikian acknowledge the receipt of the grants from the ICTP Affiliated Center Program AF-04 and the CS MES RA in the frame of the research project No. SCS 18T-1C155.The authors are also grateful to prof. M. Jaščur, J. Strečka, H. Poghosyan, andV. Abgaryan for their useful discussions.

References

[1] O. Kahn, Molecular Magnetism (VCH Publishers,1993).
[2] R. L. Carlin, Magnetochemistry(Springer,1986).
[3] A. Furrer, and O. Waldmann, Rev. Mod. Phys. **85** (2013) 367.
[4] C. Lacroix, Ph. Mendels, and F. Mila, Introduction to Frustrated Magnetism(Springer, Heidelberg, 2011).
[5] S. Sachdev, Quantum Phase Transitions (Cambridge University Press, Cambridge, 2011).
[6] G. Vidal, J. I. Latorre, E. Rico and A. Kitaev, Phys. Rev. Lett. **90** (2003) 227902.
[7] B. Gu and G. Su, Phys. Rev B **75** (2007) 174437.
[8] R. Dillenschneider, Phys. RevB **78** (2008) 224413.

[9] N. B. Ivanov, J. Richter and J. Schulenburg, Phys. Rev B **79** (2009) 104412.
[10] T. Werlang, C. Trippe, G. A. P. Ribeiro and G. Rigolin, Phys. Rev. Lett **105** (2010) 095702.
[11] O. Rojas, M. Rojas, N. S. Ananikian and S. M. D. Souza, Phys. Rev A **86** (2012) 042330.
[12] J. Torrico, M. Rojas, S. M. D. Souza, O. Rojas and N. S. Ananikian,Europhys. Lett **108** (2014) 50007.
[13] J. Streˇcka, R. C. Alecio, M. Lyra and O. Rojas, J. Magn. Magn. Mater **409** (2016) 124.
[14] S. Konar, P.S. Mukherjee, E. Zangrando, F. Lloret, N.R. Chaudhuri,Angew. Chem. Int. Ed **41** (2002) 1561.
[15] N.S. Ananikian, V. V. Hovhannisyan and R. Kenna, Physica A **396** (2014) 51.
[16] V. Hovhannisyan, N. Ananikian, and R. Kenna, Physica A **453** (2016) 116.
[17] V. S. Abgaryan, N. S. Ananikian, L. N. Ananikyan and V. Hovhannisyan,Solid State Comm **224** (2015) 15.
[18] J. A. Sheikh, A. Adhikary, H. S. Jena, S. Biswas, and S. Konar, Inorg.Chem **53** (2014) 1606.
[19] B. A. Breeze, M. Shanmugam, F. Tuna, and R. E. P. Winpenny, Chem.Commun (2007) 5185.
[20] P. Khuntia, M. Mariani, A. V. Mahajan et al., Phys. RevB **84** (2011) 184439.
[21] J. Goura, I. Oyarzabal, E. Colacio, and V. Chandrasekhar, Eur. J. Inorg.Chem (2015) 5601.
[22] X. Bao, W. Liu, L. L. Mao, S. D. Jiang, J. L. Liu, Y. C. Chen, and M. L.Tong, Inorg. Chem **52** (2013)6233.
[23] P. Kalita, J. Goura, J. M. Herrera, E. Colacio and V. Chandrasekhar, ACSOmega **3** (2018) 5202.
[24] K. Karľova, J. Strečka, and J. Richter, J. Phys.: Condens. Matter **29** (2017) 125802.
[25] K. Karľova, and J. Strečka, J. Low Temp. Phys **187** (2017) 727.
[26] J. Strečka and K. Karľova, AIP Advances **8** (2018) 101403.
[27] J. Strečka, J. Richterb, O. Derzhko, T. Verkholyakc, K. Karľová, PhysicaB **536** (2018) 364.
[28] J. Strečka, K. Karľová, Vasyl Baliha and O. Derzhko, Phys. RevB **98** (2018) 174426.
[29] H. Arian Zad and N. Ananikian, J. Phys. Condens. Matt **29** (2017) 455402.
[30] X. Y. Feng, G. M. Zhang and T. Xiang, Phys. Rev. Lett **98** (2007) 087204.
[31] S. N. Saadatmand, B. J. Powell and I. P. McCulloch, Phys. Rev B **91** (2015)245119.
[32] J.S. Valverde, O. Rojas and S. M. de Souza, J. Phys.Condens. Matt. **20**(2008) 345208.
[33] N. S. Ananikian, L. N. Ananikyan, L. A. Chakhmakhchyan and O. Rojas,J. Phys.Condens. Matt **24** (2012) 256001.
[34] V. S. Abgaryan, N. S. Ananikian, L. N. Ananikyan and V. Hovhannisyan,Solid State Comm **203** (2015) 5.
[35] O. Rojas, M. Rojas, S. M. D. Souza, J. Torrico, J. Strecka and M. L. Lyra,Physica A**486** (2017) 367.
[36] H. Arian Zad and N. Ananikian, J. Phys. Condens. Matt **30** (2018) 165403.
[37] V. M. L. D. Prasad Goli, S. Sahoo, S. Ramasesha and D.Sen, J. PhysCondens. Matt **25** (2013) 125603.
[38] S. Sahoo, V. M. L. D. Prasad Goli, D.Sen and S. Ramasesha, J. Phys.Condens. Matt **26** (2014) 276002.
[39] G. Giri, D. Dey, M. Kumar, S. Ramasesha, and Z. G. Soos, Phys. Rev B **95** (2017) 224408.
[40] V. Hovhannisyan, J. Strecka and N. Ananikian, J. Phys.Condens. Matt **28** (2016) 085401.
[41] A. Furrer, F. Juranyi, K. W. Kraemer, M. Schneider, and Th. Straessle,Phys. Rev B **83** (2011) 024404.
[42] H. J. , E. J. Kan, M.-H. Whangbo, C. Lee, Su-Huai Wei, and X. G. Gong,Phys. Rev B **83** (2011) 174402.
[43] B. Bauer, L. D. Carr, H.G. Evertz et al., J. Stat. Mech (2011) P05001.
[44] A. F. Albuquerque, et al.,J. Magn. Magn. Mater **310** (2007) 1187.